Aircraft Unsteady Aerodynamic Hybrid Modeling based on State-space Representation and Neural Network

Ouyang Guang, Lin Jun and Zhang Ping
Science and Technology on Aircraft Control Laboratory, Beihang University, XueYuan Road 37, Beijing, China

Keywords: Unsteady Aerodynamics, State-space Representation, Back-propagation Neural Network, Parameter Identification, Model Optimization.

Abstract: This paper proposes a hybrid model which combines state-space representation and back-propagation neural network to describe the aircraft unsteady aerodynamic characteristics. Firstly, the state-space model is analysed and evaluated using wind-tunnel experimental data. Subsequently, back-propagation neural network is introduced and combined with state-space representation to form a hybrid model. In this hybrid model, the separation point model in state-space representation is reserved to describe the time delay of the unsteady aerodynamic responses, while the conventional polynomial model is replaced by back-propagation neural network to improve accuracy and universality. Finally, lift coefficient and pitch moment coefficient data from the wind-tunnel experiments are used to estimate the hybrid model. With high similarity to the wind-tunnel data, the hybrid model presented in this paper is proved to be accurate and effective for aircraft unsteady aerodynamic modeling.

1 INTRODUCTION

The increasing agility requirements of modern aircrafts have invoked the development of the unsteady aerodynamic models. When flights are limited within a certain envelope of angle of attack, the traditional linear aerodynamic model is effective enough due to the incoherence between aerodynamic characteristics and the movement process. However, as the high angles of attack region becomes more accessible for modern aircrafts, the problem of adequate mathematical modeling of aerodynamic characteristics at separated and vortex breakdown flow conditions arises (Goman et al., 1994). Considering the significant role that unsteady aerodynamic forces and moments play in aircraft stability and maneuver control, efficient and universal unsteady aerodynamic modeling methods are in urgent demand.

According to (Greenwel et al., 2004), a wide range of nonlinear unsteady aerodynamic modeling techniques have been developed in recent years. For instance, in (Goman et al., 1994), the authors put forward the state-space representation of aerodynamic characteristics of an aircraft at high angles of attack. Thereafter, state-space model and modified state-space model are also adopted by (Zakaria et a., 2015) and (Williams et al., 2015) to model two-dimensional airfoils and lift hysteresis separately. Analogously, (Kumar et al., 2012) adopts steady-state stall model for nonlinear modeling. In (Chen et al., 2004), Volterra series model is used in nonlinear unsteady aerodynamics investigation.

Development of neural network has recently led to significant progress in the unsteady aerodynamic modeling field (Wang et al., 2010). With high modeling accuracy and expandability to multiple variables, neural networks have become a hot topic in unsteady aerodynamic modeling field. Several studies have been conducted recently in unsteady aerodynamic neural network modeling. The researchers in (Kumar et al., 2011) use neural Gauss–Newton method to study longitudinal aerodynamic modeling. Support vector machines model is adopted for unsteady aerodynamic modeling in (Wang et al., 2015). Feed-forward and recurrent architectures neural networks are studied and compared in (Ignatyev et al., 2015).

Although unsteady aerodynamic modeling has been studied for many years, there is still no universal solution for different aircrafts due to limited understanding of the flow mechanism. At the time of this writing, there is still no standard

Guang, O., Jun, L. and Ping, Z.
Aircraft Unsteady Aerodynamic Hybrid Modeling Based on State-Space Representation and Neural Network.
DOI: 10.5220/0005691702320239
In *Proceedings of the 5th International Conference on Pattern Recognition Applications and Methods (ICPRAM 2016)*, pages 232-239
ISBN: 978-989-758-173-1

unsteady aerodynamic model. However, some attempts are still proved to be of great value. For example, the state-space model can represent time delay characteristics, which reasonably describes actual physical mechanism of wing flow separation and reattachment. Relatively, neural network model can serve as universal approximators for unknown aircraft systems and be easily extended to multi-axis motions modeling. Therefore, an intuitive and meaningful attempt is to combine these two models and get an unsteady aerodynamic hybrid model with all these advantages.

This paper is organized as follows: In Section 2, aircraft unsteady aerodynamic mechanism is discussed. Subsequently, state-space model is introduced and evaluated using the wind-tunnel experimental data. Section 3 describes the back-propagation neural network and the hybrid unsteady aerodynamic model. Nested parameter optimization algorithm for the hybrid model is also given in this section. In Section 4, the hybrid model is finally validated with lift coefficient and pitch moment coefficient data which come from the wind-tunnel experiments.

2 STATE-SPACE PRESENTATION

2.1 Unsteady Aerodynamic Mechanism

As a key factor of unsteady aerodynamic modeling, mechanism research has a significant impact on model validation. According to (Sun et al., 2015), unsteady flow separation vortices at the trailing edge are the causes of the unsteady aerodynamic characteristics. During maneuvers, the wing flow separates and reattaches. As adjustment process of the surface vortex has dynamic time delay characteristic, the aerodynamic forces and moments show obvious unsteady phenomena. For example, pneumatic hysteresis loop can be seen from the wind-tunnel data of the longitudinal forced pitch oscillations in Fig. 1.

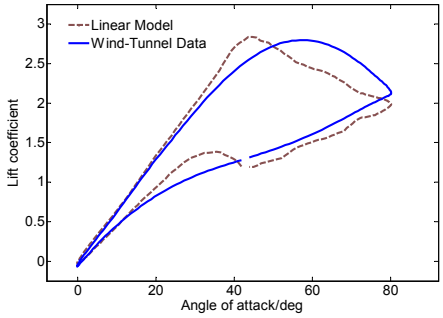

Figure 1: Linear aerodynamic model.

Linear model is a conventional aerodynamic model. In many practical cases, the aerodynamic forces and moments are approximated by linear terms in their Taylor series expansions. In the case of lift coefficient, the function is defined as follows:

$$C_L = C_{Ls}(\alpha) + C_{Lq}(\alpha)\frac{q\bar{c}}{2V} + C_{L\dot{\alpha}}(\alpha)\frac{\dot{\alpha}\bar{c}}{2V} \quad (1)$$

Where C_L is the total lift coefficient, C_{Ls} denotes the static lift coefficient. α, q are angle of attack and pitch angle rate separately. $C_{Lq}, C_{L\dot{\alpha}}$ are corresponding dynamic factors. V presents air speed, $\bar{c}$ is the wing mean geometric chord. Linear model assumes that aerodynamic forces and moments depend only on the instantaneous values of the flight states. Due to lacking the considerations of unsteady aerodynamic effects, the outputs of linear model often contain notable error at high angles of attack comparing to the wind-tunnel data (Fig. 1).

2.2 State-space Model

The state-space model takes time delay of flow separation and reattachment into account. An internal variable which describes the flow state is introduced by (Goman et al., 1994) to express time delay of unsteady aerodynamics at high angles of attack. This internal state variable is called the longitudinal position of the separation point x. The movement of the separation point for unsteady flow conditions is defined as follows:

$$\begin{aligned} x_0(\alpha) &= \frac{1}{1+e^{\sigma(\alpha-\alpha^*)}} \\ \tau_1 \frac{dx}{dt} + x &= x_0(\alpha - \tau_2\dot{\alpha}) \end{aligned} \quad (2)$$

Function $x_0(\alpha)$ is the static variation which depends on the instantaneous angle of attack α. α^* is defined as the angle of attack when separation point reaches the middle of airfoil chord, σ is slope factor.

The unsteady fluid mechanics processes are divided into two groups. The first group is the quasi-steady effects such as circulation and boundary-layer convection lags, which tend to delay flow separation or burst onset by an amount roughly proportional to the pitch rate. This combined effect is expressed as an argument shift $x_0(\alpha - \tau_2\dot{\alpha})$. Where the parameter τ_2 defines the total time delay associated with the above effects. The second group of flow phenomena

define the transient aerodynamic effects, in which any disturbance of the separated flow is followed by an adjustment or relaxation back to the steady-state. The adjustment process is governed by a first-order ordinary differential equation (Formula 2) with relaxation time constant τ_1.

The solid line and dashed lines show the variations of the separation point position for steady and unsteady conditions separately in Fig. 2. The difference between solid line and dashed lines causes the pneumatic hysteresis of unsteady aerodynamics.

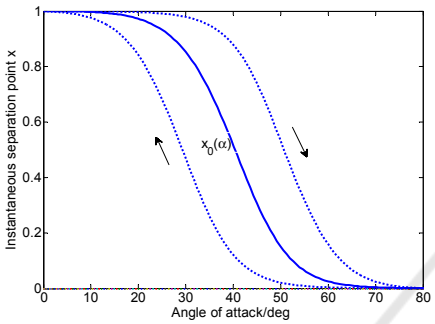

Figure 2: Instantaneous separation point variations.

In state-space model, aerodynamic forces and moments depend on not only the instantaneous values of the flight states, but also the instantaneous separation point position that can differ considerably from its stationary value. Since the pitch oscillations are considered with $q = \dot{\alpha}$, the effects of $\dot{\alpha}$ are no longer included in the subsequent longitudinal unsteady aerodynamic coefficient expressions. The corresponding unsteady lift coefficient state-space representation is:

$$C_L = C_{Ls}(\alpha) + C_{Ld}(\alpha, q, x) \tag{3}$$

The static coefficient C_{Ls} is conventionally approximated with the first three items in its Taylor series expansion, while the dynamic coefficient C_{Ld} is approximated with the first five items in its Taylor series expansion.

$$\begin{aligned} C_{Ls} &= C_{Ls0} + C_{Ls\alpha}(x_0)\alpha + C_{Ls\alpha^2}(x_0)\alpha^2 \\ C_{Ld} &= C_{L\alpha}(x)\alpha + C_{Lq}(x)\frac{q\bar{c}}{2V} + C_{L\alpha^2}(x)\alpha^2 + \\ &\quad C_{Lq^2}(x)\frac{q^2\bar{c}}{2V} + C_{L\alpha q}(x)\alpha\frac{q\bar{c}}{2V} \end{aligned} \tag{4}$$

All the corresponding factors in both the static coefficient and the dynamic coefficient can be expressed with second-order polynomial functions, like $C_{Ls\alpha}$ and $C_{L\alpha}$ in the lower formula.

$$\begin{aligned} C_{Lsa}(x_0) &= k_{Ls\alpha 0} + k_{Ls\alpha 1}x_0 + k_{Ls\alpha 2}x_0^{\,2} \\ C_{L\alpha}(x) &= k_{L\alpha 0} + k_{L\alpha 1}x + k_{L\alpha 2}x^2 \end{aligned} \tag{5}$$

Where $k_{Ls\alpha 0}, k_{Ls\alpha 1}, k_{Ls\alpha 2}$ and $k_{L\alpha 0}, k_{L\alpha 1}, k_{L\alpha 2}$ are unknown parameters in the polynomial aerodynamic model. Totally, 26 parameters should be determined for the lift coefficient state-space representation, including four parameters $\sigma, \alpha^*, \tau_1, \tau_2$ in the separation point model (Formula 2) and all the relevant factors in the polynomial model (Formula 5).

2.3 State-space Model Evaluation

Suitable simulations of the maneuvers in the wind tunnels are important for understanding the physics of complex flow phenomena (Hosder et al., 2007). These maneuvers should allow the physical simulation of aircraft dynamic behavior, which is subject to the dynamic similarity of the aircraft model, and identification of the aircraft aerodynamic model structure and its parameters (Pattinson et al., 2013). For the case of symmetrical motion of the wing in the longitudinal plane, pitch-only oscillation has been successfully used to characterize unsteady aerodynamics at high angles of attack (Pattinson et al., 2012). In this paper, Forced large-amplitude pitch oscillations are executed in the wind tunnel. The corresponding experimental data of aerodynamic forces and moments are collected and used to estimate the aerodynamic models.

Harmonic motions in pitch oscillations with a fixed center of gravity are implemented:

$$\begin{aligned} \alpha &= \alpha_0 - A\sin(2\pi ft) \\ \dot{\alpha} &= q = -2\pi fA\cos(2\pi ft) \end{aligned} \tag{6}$$

Oscillations were carried out with amplitude $A = 40^o$ and different pitching frequencies f. The initial angle of attack α_0 is set to 40^o, so the angle of attack α varies from 0^o to 80^o. Lift coefficient and pitch moment coefficient data at $f = 0.4Hz$, $f = 0.6Hz$ and $f = 0.8Hz$ are used to testify the validity of the state-space model. After a proper parameter optimization for lift and pitch moment state-space models with Nelder-Mead method and particle swarm optimization method, the comparisons between optimized state-space model and corresponding wind-tunnel data are partly shown in the following figures:

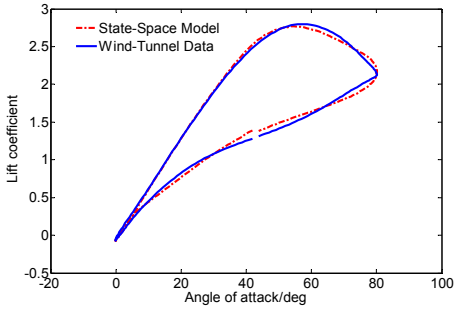

Figure 3: Lift coefficient response at f=0.6Hz.

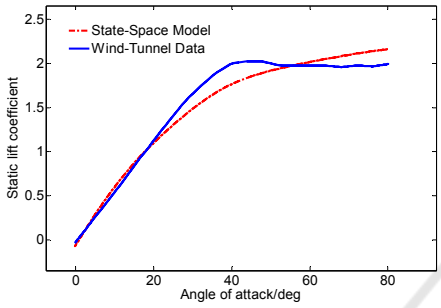

Figure 4: Static lift coefficient response.

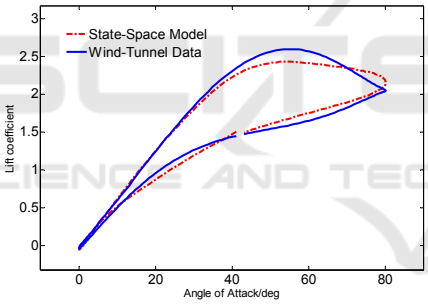

Figure 5: Lift coefficient response at f=0.4Hz.

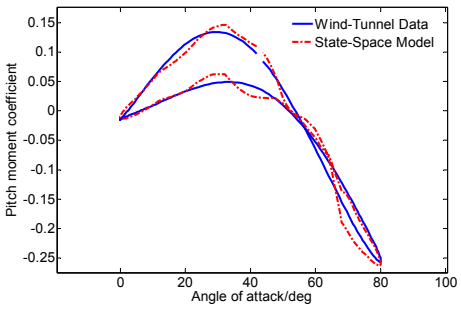

Figure 6: Pitch moment coefficient response at f=0.6Hz.

The figures above reveal that state-space model can approximate the wind-tunnel experimental data to a certain extent. Fig. 5 and Fig. 6 show that though state-space model can effectively reflect time delay characteristics of unsteady aerodynamics at high angles of attack, the model responses are not always in good agreement with the wind-tunnel data. The polynomial model is not accurate enough to describe the nonlinear static aerodynamic coefficient, like the static lift coefficient in Fig. 4.

Goman's nonlinear differential equation concept provides the most promising combination of relative simplicity, retention of physical significance in its parameters, and ability to model a wide range of common flow features (Greenwel et al., 2004). However, modifications should be added to state-space model to capture more accurate and reliable unsteady aerodynamic responses.

3 HYBRID MODEL

Neural networks (NN) have recently been shown to be an effective tool for modeling nonlinear unsteady aerodynamics regardless of the aircraft configurations. In previous studies, a simple time delay is generally added to the flight states instantaneous values as the input signals in unsteady aerodynamic NN model. Though sometimes these NN models can achieve good accuracy due to the excellent approximating performance, actual physical mechanism of unsteady aerodynamics is not clearly reflected and the NN models are usually oversized with redundant neurons. As a meaningful attempt in this paper, a hybrid model which combines state-space representation and back-propagation neural network is presented to integrate respective advantages in these two models.

3.1 Back-propagation Neural Network

Back-propagation neural networks (BPNN) are the most widely applied neural network models. The structure of generalized three-layer neural network consists of the input layer, the hidden layer and the output layer (Fig. 7). The node in the neural network is called the neuron. Each neuron receives signals from the neurons in the previous layer, and calculates its output through a specific transfer function.

Fig. 8 shows the typical neuron transfer model. For nodes in the hidden layer, input signals are $x_j (j = 1, 2, ..., n)$. These signals are summed with weight values w_j corresponding to the signal connections. Bias value s is added to the weighted sum of the input signals to generate a summed value net . The final output g of the node is mapped through a commonly used hyperbolic tangent

sigmoid transfer function as the nonlinear activation function. The nodes in the output layer share the same scheme as the nodes in the hidden layer.

$$net = \sum_{j=1}^{n} x_j w_j + s$$
$$g = f(net) = \frac{2}{1+e^{-2net}} - 1 \quad (7)$$

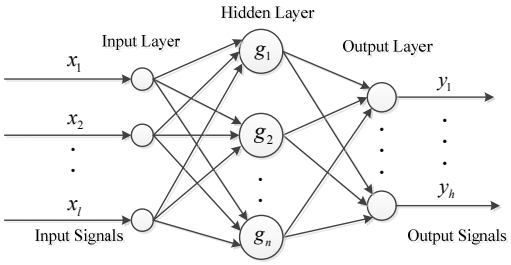

Figure 7: Generalized neural network structure.

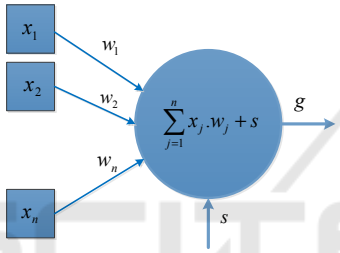

Figure 8: Typical neuron transfer model.

To minimize the mean-squared error E between BPNN model response y_{Bj} and the actual response y_{Rj}, the error value e_j is propagated backwards through the network for weight values and bias values updates.

$$\min E = \sqrt{\sum_{j=1}^{N} (y_{Bj} - y_{Rj})^2 / N} = \sqrt{\sum_{j=1}^{N} e_j^2 / N} \quad (8)$$

Gradient descent method is used in the back-propagation neural network for parameter learning. When the mean-squared error decreases and reaches a given threshold range, parameter optimization stops and the BPNN model is regarded as an acceptable approximator to the actual model.

3.2 Hybrid Model Structure

To obtain a more accurate and reliable unsteady aerodynamic model and reflect actual flow separation characteristics, the unsteady aerodynamic hybrid model is proposed in this paper. As the differential equation of the separation point can be used to simulate time delay of unsteady aerodynamic responses, the separation point model is reserved in the hybrid model. As far as model accuracy and output response approximation are concerned, back-propagation neural network is introduced to replace the conventional polynomial model. The structure of unsteady aerodynamic hybrid model is shown in the following figure.

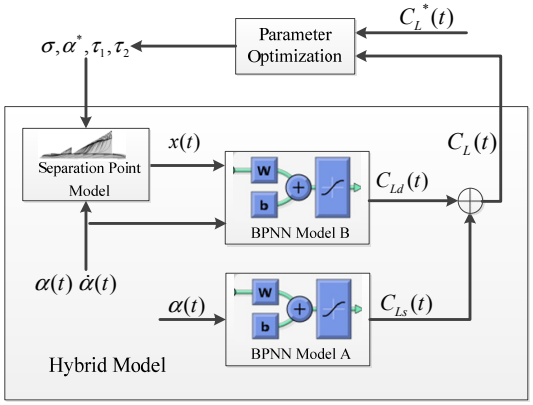

Figure 9: Unsteady aerodynamic hybrid model structure.

Fig. 9 shows that in lift coefficient unsteady hybrid model, the static lift coefficient and the dynamic lift coefficient are identified separately. As the static coefficient only depends on the angle of attack, a simple BPNN model A is adopted to describe the nonlinear steady mapping between these two variables. For the dynamic lift coefficient, the separation point model is firstly used to generate the separation point x from α and $\dot{\alpha}$. Subsequently, BPNN model B is introduced with $\alpha, \dot{\alpha}$ and x as input signals to simulate the unsteady lift component. The dynamic lift coefficient C_{Ld} is added to the static lift coefficient C_{Ls} to form the total lift coefficient response C_L. Finally, C_L is compared to the wind-tunnel lift coefficient data to optimize the relevant parameters in the hybrid model.

3.3 Hybrid Model Optimization

Two sets of unknown parameters exist in the unsteady aerodynamic hybrid model. Four parameters $\sigma, \alpha^*, \tau_1, \tau_2$ in the separation point model decide the separation point dynamic characteristics, while all the relevant weight values and bias values in BPNN model reveal the nonlinear mapping function of the unsteady aerodynamic forces and moments. All of the above unknown parameters should be identified and optimized to realize the best model response.

For the unknown values in BPNN model A, a direct gradient descent method is taken to optimize the corresponding parameters. When it comes to the dynamic aerodynamic component identification, a nested parameter optimization algorithm is used. The four parameters $\sigma, \alpha^*, \tau_1, \tau_2$ are optimized as the outside loop of the nested optimization structure, the corresponding optimization algorithms are Nelder-Mead method and particle swarm optimization method. The relevant weight values and bias values in BPNN model B are identified with gradient descent method as the inner loop. The nested parameter optimization structure is as follows:

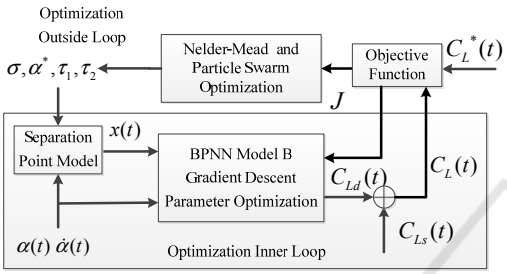

Figure 10: Nested parameter optimization structure.

In the case of dynamic lift coefficient identification, the optimal objective function is defined as the mean-squared error between the hybrid model response and the wind-tunnel data, as shown in the following formula.

$$\min J = \sqrt{\sum_{j=1}^{N} (C_{Lj} - C_{Lj}^*)^2 / N} \quad (9)$$

As far as the number of the hidden layer neurons is concerned, an oversized network could overfit and overlearn for a special data set. Conversely, an undersized network with too few hidden layer neurons could significantly reduce the results accuracy (Boëly et al., 2010). For the parameter identification of the hybrid model, a large enough integer value is chosen as the number of the hidden layer neurons to ensure the model response accuracy. After the parameters $\sigma, \alpha^*, \tau_1, \tau_2$ are determined with the oversized BPNN model B, a model simplification process is executed to reduce the redundant neurons. Useless and redundant neurons are deleted one-by-one and the parameters in BPNN model B are readjusted until the mean-squared error J exceeds the pre-determined threshold. Finally, a simplified hybrid model is achieved without lowering model accuracy criterion.

4 SIMULATION RESULTS

The considered unsteady aerodynamic hybrid model is tested using the wind-tunnel experimental data. As it is mentioned in Section 2, the lift coefficient and pitch moment coefficient data come from the forced large-amplitude pitch oscillations at $f = 0.4Hz$, $f = 0.6Hz$ and $f = 0.8Hz$. Two thirds of the experimental data are used to train the neural networks in the hybrid model, and one third of the experimental data are used to evaluate the hybrid model performance.

For the hidden layer in BPNN model A, 6 neurons are enough to create a more accurate static aerodynamic model comparing to state-space model. The responses of the static BPNN models are illustrated in Fig. 11 and Fig. 12.

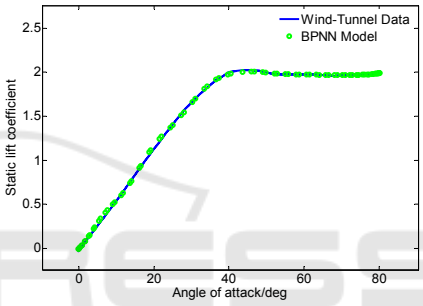

Figure 11: Static lift coefficient response.

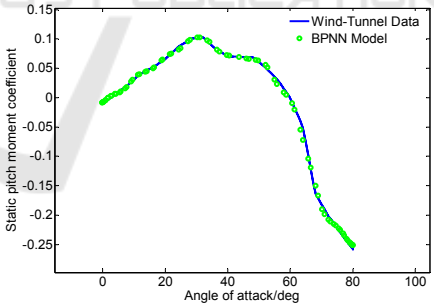

Figure 12: Static pitch moment coefficient response.

As for the identifications of the dynamic aerodynamic component, 30 hidden layer neurons are set as the initial size of BPNN model B. The four parameters $\sigma, \alpha^*, \tau_1, \tau_2$ are firstly identified using the nested optimization algorithm mentioned in Section 3.

Table 1: Identification results in separation point model.

σ	α^* / deg	τ_1 / s	τ_2 / s
0.11	41.2	0.042	0.047

Subsequently, model simplification process is carried out to reduce the redundant neurons. The simplification results indicate that 6 hidden layer neurons are accurate enough to represent the nonlinear mapping relation in BPNN model B for lift coefficient modeling. As for the pitch moment coefficient, 7 hidden layer neurons are necessary to guarantee model accuracy. The optimized unsteady aerodynamic hybrid models are compared with the conventional state-space models. The mean-squared errors J are listed in Table 2. SS-M is short for state-space model, CH-M denotes the complicated hybrid model with 30 hidden layer neurons, SH-M represents the simplified hybrid model.

Table 2: Mean-squared error comparisons.

J / 10^{-2}		f=4Hz	f=6Hz	f=8Hz
Lift coefficient	SS-M	7.87	4.58	8.66
	CH-M	3.05	1.34	2.47
	SH-M	3.32	1.61	3.46
Pitch moment coefficient	SS-M	4.79	4.12	11.1
	CH-M	0.42	0.35	0.40
	SH-M	1.05	0.56	0.57

Comparing to conventional state-space model, the hybrid model can achieve obvious accuracy improvement in approximating the unsteady aerodynamic response. The response results of the simplified hybrid models achieve good agreements with different wind-tunnel experimental data, which are illustrated in the following figures.

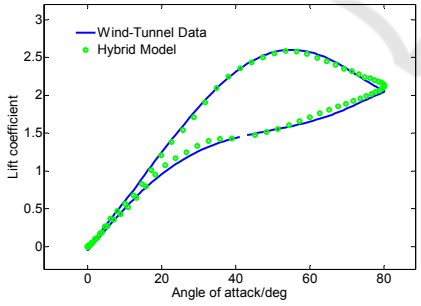

Figure 13: Lift coefficient response at f=0.4Hz.

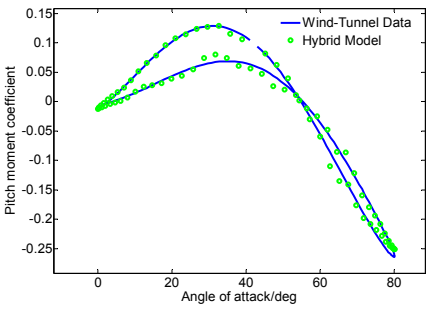

Figure 14: Pitch moment coefficient response at f=0.4Hz.

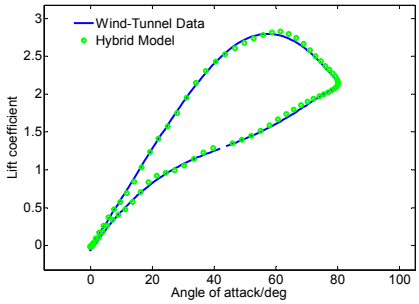

Figure 15: Lift coefficient response at f=0.6Hz.

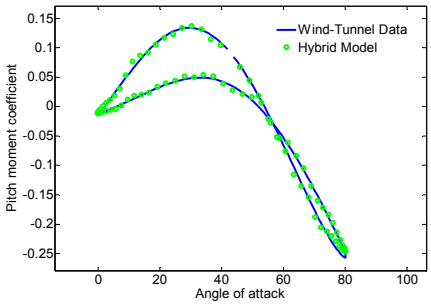

Figure 16: Pitch moment coefficient response at f=0.6Hz.

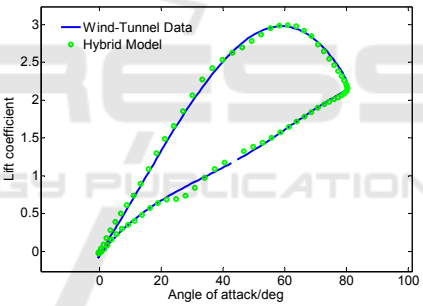

Figure 17: Lift coefficient response at f=0.8Hz.

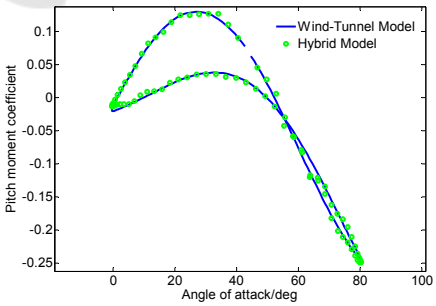

Figure 18: Pitch moment coefficient response at f=0.8Hz.

5 CONCLUSIONS

A hybrid model which combines state-space representation and back-propagation neural network

is proposed in this paper to describe the aircraft unsteady aerodynamic characteristics. According to the simulation results, the conventional state-space model has limited approximation quality in modeling unsteady aerodynamics. For the purpose of improving model accuracy and universality, back-propagation neural network is introduced and replaces the polynomial model in state-space representation. The unsteady aerodynamic hybrid model is identified and optimized with nested optimization algorithm using the wind-tunnel data in forced large-amplitude pitch oscillation experiments. With satisfactory similarity to the wind-tunnel data, the hybrid model presented in this paper is validated to be effective in both reflecting unsteady time delay characteristics and representing complex nonlinear mapping relation for unsteady aerodynamics at high angles of attack.

ACKNOWLEDGEMENTS

This work was made possible thanks to the support of Science and Technology on Aircraft Control Laboratory.

REFERENCES

Boëly, N., Botez, R. M., 2010. New approach for the identification and validation of a nonlinear F/A-18 model by use of neural networks. *IEEE Transactions on Neural Networks*, 21(11):1759–1765.

Chen, G., Xu, M., and Chen, S. L., 2004. Reduced-order model based on volterra series in nonlinear unsteady aerodynamics. *Journal of Astronautics*, 25(5): 492–295.

Goman, M., Khrabrov, A., 1994. State-space representation of aerodynamic characteristics of an aircraft at high angles of attack. *Journal of Aircraft*, 31(5):1109-1115.

Greenwell, D. I., 2004. A Review of Unsteady Aerodynamic Modeling for Flight Dynamics of Manoeuvrable Aircraft. In *AIAA Atmospheric Flight Mechanics Conference and Exhibit*, Paper 2004-5276.

Hosder, S., Simpson, R. L., 2007. Experimental investigation of unsteady flow separation on a maneuvering axisymmetric body. *Journal of aircraft*, 44(4): 1286–1295.

Ignatyev, D. I., Khrabrov, A. N., 2015. Neural network modeling of unsteady aerodynamic characteristics at high angles of attack. *Aerospace Science and Technology*, 41: 106–115.

Kumar, R., Ghosh, A. K., 2011. Nonlinear Longitudinal Aerodynamic Modeling Using Neural Gauss-Newton Method. *Journal of Aircraft*, 48(5): 1809–1813.

Kumar, R., Mishra, A., Ghosh, A. K., 2012. Nonlinear Modeling of Cascade Fin Aerodynamics Using Kirchhoff's Steady-State Stall Model. *Journal of Aircraft*, 49(1): 315–319.

Pattinson, J., Lowenberg, M. H., Goman, M. G., 2012. Multi-Degree-of-Freedom Wind-Tunnel Maneuver Rig for Dynamic Simulation and Aerodynamic Model Identification. *Journal of Aircraft*, 50(2): 551–566.

Pattinson, J., Lowenberg, M. H., Goman, M. G. 2013. Investigation of Poststall Pitch Oscillations of an Aircraft Wind-Tunnel Model. *Journal of Aircraft*, 50(6): 1843–1855.

Sun, W., Gao, Z., Du, Y., Xu, F., 2015. Mechanism of unconventional aerodynamic characteristics of an elliptic airfoil. *Chinese Journal of Aeronautics*, 28(3): 687–694.

Wang, B. B., Zhang, W. W., Ye, Z. Y., 2010. Unsteady Nonlinear Aerodynamics Identification Based on Neural Network Model. *Acta Aeronautica Et Sinica*, 31(7): 1379–1388.

Wang, Q., Qian, W., He, K., 2015. Unsteady aerodynamic modeling at high angles of attack using support vector machines. *Chinese Journal of Aeronautics*, 28(3): 659–668.

Williams, D. R., Reißner, F., Greenblatt, D., Müller-Vahl, H., Strangfeld, C., 2015. Modeling Lift Hysteresis with a Modified Goman-Khrabrov Model on Pitching Airfoils. In *45th AIAA Fluid Dynamics Conference*, Paper 2015-2631.

Zakaria, M. Y., Taha, H. E., Hajj, M. R., Hussein, A. A., 2015. Experimental-Based Unified Unsteady Nonlinear Aerodynamic Modeling For Two-Dimensional Airfoils. In *33rd AIAA Applied Aerodynamics Conference*, Paper 2015-3167.